The Abdus Salam
International Centre
for Theoretical Physics

United Nations
Educational, Scientific and
Cultural Organization

IAEA
International Atomic Energy Agency

2444-5

College on Soil Physics - 30th Anniversary (1983-2013)

25 February - 1 March, 2013

THE SIMILARITY CONCEPT OF PREVEDELLO FOR THE ANALYSIS OF WATER INFILTRATION INTO SOILS

REICHARDT Klaus and Nielsen D.R.
CENA Centro de Energia Nuclear Na Agricultura
Universidade de Sao Paulo, Av. Centenario 303
Sao Dimas, CP 96, SP 13400-970 Piracicaba
BRAZIL

THE SIMILARITY CONCEPT OF PREVEDELLO FOR THE ANALYSIS OF WATER INFILTRATION INTO SOILS

Klaus Reichardt[1], Donald R. Nielsen[2]

[1] Soil Physics Laboratory, Center for Nuclear Energy in Agriculture (CENA), University of São Paulo (USP), Piracicaba, SP, Brazil. E-mail: klaus@cena.usp.br
[2] Professor at UCD, Davis, California, USA.

Introduction

The process of infiltration of water into homogeneous soils is well described in the literature. It is an important process for about all soil water management projects or studies. Its solution is based on Richards equation, which includes very non linear functions, like the soil water retention curve and the soil hydraulic conductivity function. Therefore analytic solutions of the infiltration process are extremely complex and today numerical procedures took an important role in this problem. However, a single solution for processes occurring in soils of different characteristics remains a lingering challenge for soil scientists. Here, that challenge is discussed for horizontal water infiltration considering the similarity of soil hydraulic characteristics among all kinds of soils.

The illustration shown below for the infiltration process serves as an introduction for the understanding of Prevedello´s similarity concept:

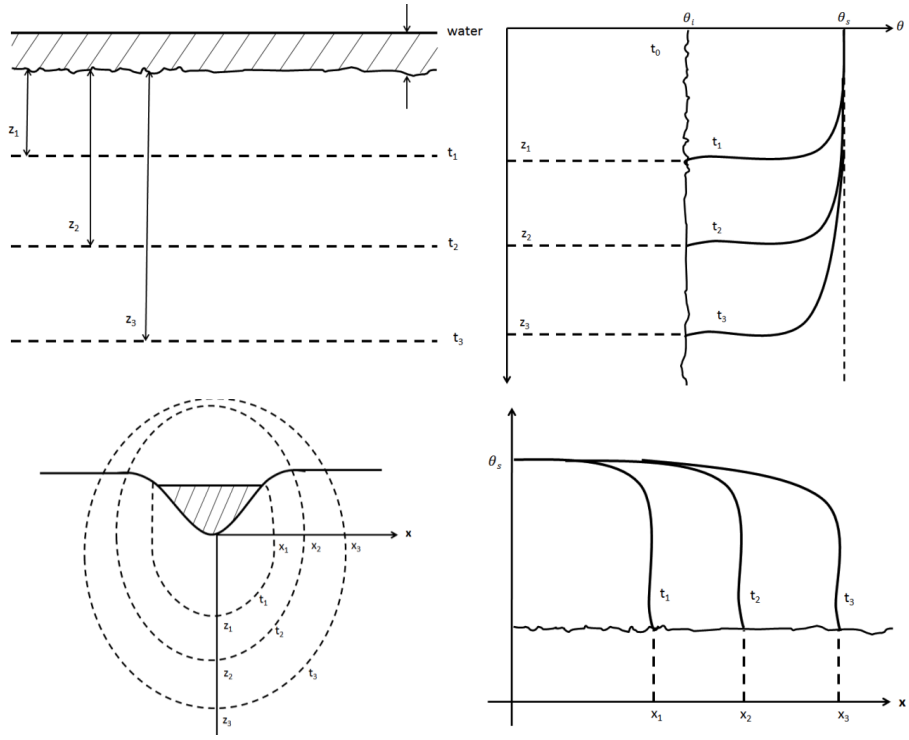

Figure 000. Shallow ponding and furrow infiltrations.

Green and Ampt (1911)

Much before soil physics developed to a solid description of soil water phenomena, Green and Ampt published a solution to the infiltration process, which is useful to date in practical field problems. They simply assumed that the soil water infiltration profiles shown above are rectangular, admitting that the water movement was like a steady piston flow. In this way, they could solve the already available Darcy flow equation, and obtain their solution:

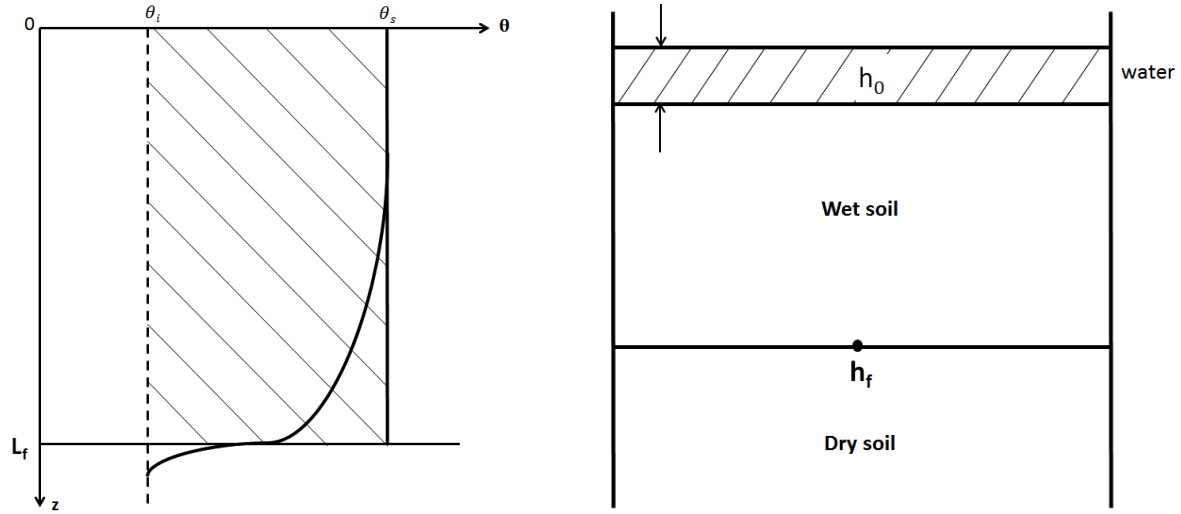

Figure 00. Green and Ampt assumptions.

$$i = \frac{dI}{dt} = -K_s \frac{h_0 + L_f(t)}{L_f(t)}$$

where i = infiltration rate, I = cumulative infiltration, K_s = saturated hydraulic conductivity.

$$I = [2K_s (h_0 - h_f)\Delta\theta]^{1/2} * t^{1/2}$$

where $\Delta\theta = (\theta_s - \theta_i)$.

Similarity concept of Prevedello

Based on the classical concepts of Darcy (1856), Boltzmann (1894), Buckingham (1907), Green and Ampt (1911) and Richards (1931), countless equations have been analytically solved to describe the infiltration of water into soils satisfying specific initial and boundary conditions. Today, exact and approximate solutions of Richards' equation for a homogeneous, semi-infinite soil column being infiltrated with water under the following initial and boundary conditions are commonplace in soil physics and soil hydrology textbooks:

$$\theta = \theta_i \qquad x \geq 0 \qquad t = 0$$
$$\theta = \theta_0 \qquad x = 0 \qquad t > 0$$
$$\theta = \theta_i \qquad x \to \infty \qquad t > 0$$

Based on the fact that **shapes of the soil water retention curves and of the infiltration soil water content profiles** are very similar, i.e., one being a mirror image of the other

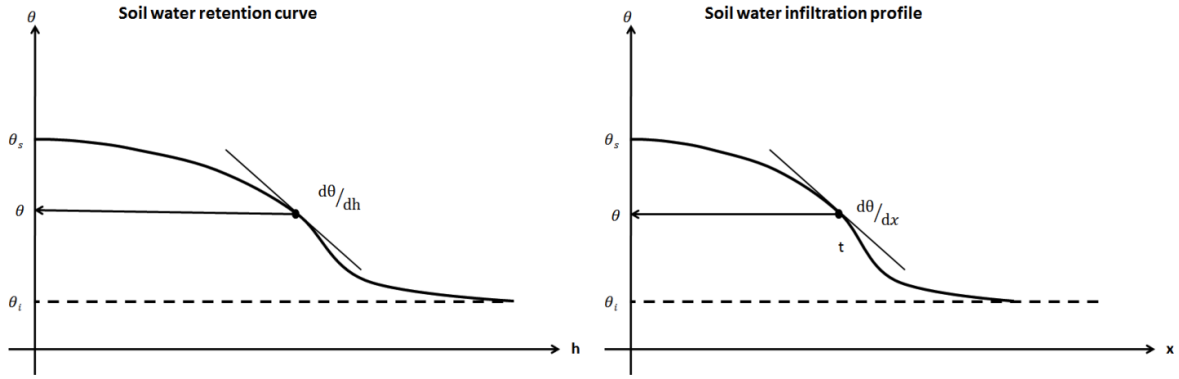

Figure 0. Schematic explanation of the similarity (mirror) hypothesis of Prevedello.

Prevedello et al (2008) assumed that the derivatives of these functions could be taken as equal. More formally the similarity hypothesis developed by Prevedello to estimate the horizontal infiltration of water into homogeneous soils was based on the classical Richards' equation together with an extension of the historic Boltzmann transform function. Their similarity hypothesis illustrated in Figure 1A relates the soil water retention function $\theta(h)$ to an extended Boltzmann transform function $\theta(\lambda^N)$ by the equation

$$\lambda^N \frac{d\theta}{d\lambda^N} = h \frac{d\theta}{dh} \qquad [1]$$

where they selected $N = 2$ and used experimental data of a marine sand. Although their introduction of the similarity hypothesis was easily understood and readily accepted, its mathematical development was slightly robust and its application very limited. Being aware of the necessity of a more comprehensive methodology, they acknowledged that the applicability of their similarity hypothesis remained open for future research – both theoretical and experimental.

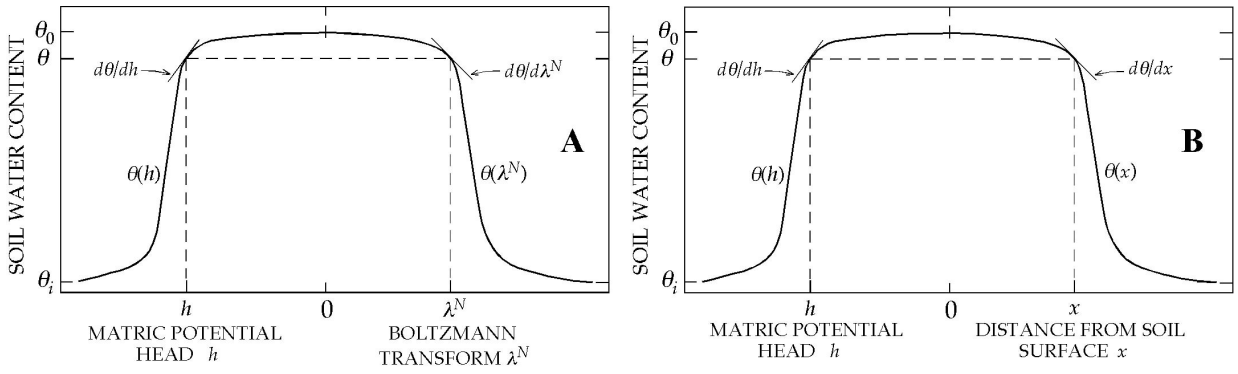

Figure 1. Diagrams of similarity hypotheses relating the soil water retention function $\theta(h)$ to a generalized Boltzmann transform $\theta(\lambda^N)$ and to the distribution of θ in the soil profile. θ_i is the initial soil water content throughout the soil and θ_0 the water content at the soil surface for $t > 0$.

Next, Prevedello et al. (2009) published a second similarity solution – for water infiltrating vertically downward, vertically upward and horizontally into the same marine sand. They assumed, "during infiltration, the shape of the soil water content profile can be visualized as a mirror image of the soil water retention curve" (Figure 1B). Although they explicitly stated that this second assumption was, "similar but not the same as that of Prevedello et al. (2008)", they did not identify a functional relationship between a Boltzmann transform and h in 2009. However, within a year, Prevedello and Loyola (2010) endeavored to show that the mathematical development of both similarity analyses (2008 and 2009) depended upon an identical equation to quantify the matric potential head gradient. Their effort hinged on an analysis of a generalization of the similarity existing between $\theta(\lambda^N)$ and $\theta(h)$ for different values of N as illustrated in Figure 1A. They emphasized that the gradient $\partial h / \partial x$ being equal to $2h/x$ as initially hypothesized by Prevedello et al. (2008) for $N = 2$ is always simplified from $2h/x$ to h/x during the derivation of the infiltration solution. They should have emphasized that the gradient $\partial h / \partial x$ equals $2h/x$ and remains $2h/x$. And for that particular similarity assumption, the mean value of the gradient is h/x and remains h/x. Although Prevedello and Loyola stated that the similarity solution published by Prevedello et al. (2009), "presupposes a relation of the type $\lambda^N = C_N h$ with $N = 1$", they did not provide such a solution nor did they unmistakably verify their presumption.

Our primary objective in this manuscript is to improve the utility of similarity concepts in Richards' equation to describe water infiltrating into homogeneous soils. First, we provide a similarity solution explicitly based on the classical Boltzmann transform having a unit exponent (Illustrated in Figure 1A when $N = 1$). Next we annotate the publications of Prevedello et al. (2008 and 2009) and Prevedello

and Loyola (2010), and finally, we briefly examine the utility of similarity hypotheses applied to quantitative infiltration experiments conducted on homogeneous columns of Columbia silt loam and Hesperia sandy loam – soils more universally typical than the marine sand used by them or a strongly aggregated soil as suggested by them.

A Hypothetical Similarity Solution Using the Classical Boltzmann Transform *l*

Integrating integrals with indefinite limits

We begin by selecting a unit exponent for *l* (*N* = 1) in Eq. [1] in order to invoke the classical Boltzmann transform $\lambda(\theta) = xt^{-1/2}$ into the similarity hypothesis. Hence, we have

$$\frac{d\lambda}{\lambda} = \frac{dh}{h} \qquad [2]$$

which when integrated with indefinite limits

$$\int \frac{d\lambda}{\lambda} = \int \frac{dh}{h} + \ln\beta_1$$

yields $\lambda = \beta_1 h$ where b_1 is the constant of integration having a value dependent upon the boundary conditions of both *l* and *h* used to solve Richards' equation

$$\frac{\partial\theta}{\partial t} = \frac{\partial}{\partial x}\left[K(h)\frac{\partial h}{\partial x}\right].$$

Differentiating

$$\frac{d\theta}{dh}\frac{\partial h}{\partial t} = K(h)\frac{\partial^2 h}{\partial x^2} + \frac{\partial h}{\partial x}\frac{\partial K(h)}{\partial h}\frac{\partial h}{\partial x} = K(h)\frac{\partial^2 h}{\partial x^2} + \frac{\partial K(h)}{\partial h}\left(\frac{\partial h}{\partial x}\right)^2$$

we obtain

$$\left.\frac{d\theta}{dh}\frac{\partial h}{\partial t}\right|_{x=\text{comstant}} = K(h)\left.\frac{\partial^2 h}{\partial x^2}\right|_{t=\text{comstant}} + \left.\frac{dK(h)}{dh}\left(\frac{\partial h}{\partial x}\right)^2\right|_{t=\text{comstant}} \qquad [3]$$

Recognizing that $\lambda[\theta(h)] = xt^{-1/2}$, $\lambda = \beta_1 h$ becomes

$$x(h,t) = \beta_1 h t^{1/2}, \qquad [4]$$

The partial derivative of Eq. [4] with respect to *t* holding *x* constant is

$$\frac{\partial h}{\partial t} = -\frac{h}{2t} \qquad [5]$$

The partial derivative of Eq. [4] with respect to *x* holding *t* constant is

$$\frac{\partial h}{\partial x} = \frac{1}{\beta_i t^{1/2}} \qquad [6]$$

The partial derivative of Eq. [6] with respect to *x* holding *t* constant is

$$\frac{\partial^2 h}{\partial x^2} = 0 \qquad [7]$$

Substituting the above partial derivatives from Eqs. [5, 6 and 7] into Eq. [3], we obtain

$$-\beta_1^2 h \frac{d\theta}{dh} = 2\frac{dK(h)}{dh} \qquad [8]$$

To obtain the value of b_1, we multiply the above equation by *Dh* to prepare for its integration between boundary conditions q_i and q_0

$$-\beta_1^2 h \frac{d\theta}{dh}\Delta h = 2\frac{dK(h)}{dh}\Delta h$$

which reduces to

$$-\beta_1^2 h \Delta\theta = 2\Delta K$$

Integrating the above equation

$$-\beta_1^2 \int_{\theta_i}^{\theta_0} h d\theta = 2\int_{K(\theta_i)}^{K(\theta_0)} dK$$

and re-arranging and taking the square root of β_1^2, we obtain

$$\beta_1 = -\sqrt{-2(K_0 - K_i) \Big/ \int_{\theta_i}^{\theta_0} h d\theta}$$

Substituting β_1 into Eq. [4], we have

$$x(h,t) = -ht^{1/2}\sqrt{-2(K_0 - K_i) \Big/ \int_{\theta_i}^{\theta_0} h d\theta} \qquad [9]$$

from which the value of *h*(*x*,*t*) becomes

$$h = \frac{x}{t^{1/2}\beta_1} = \frac{-x}{t^{1/2}\sqrt{-2(K_0 - K_i) \Big/ \int_{\theta_i}^{\theta_0} h d\theta}} \qquad [10]$$

The partial derivative of *h* holding *t* constant is

$$\frac{\partial h}{\partial x} = \frac{1}{\beta_1 t^{1/2}} = \frac{-1}{t^{1/2}\sqrt{-2(K_0 - K_i) \Big/ \int_{\theta_i}^{\theta_0} h d\theta}} \qquad [11]$$

Multiplying the above equation by -*K*(*h*), we obtain the soil water flux density within the soil at any time *t*

$$q(h,t) = \frac{K(h)}{t^{1/2}\sqrt{-2(K_0 - K_i)\Big/\int_{\theta_i}^{\theta_0} h d\theta}} \quad [12]$$

The infiltration velocity at the soil surface $q(0,t)$ [or $q_0(t)$] is merely

$$q_0 = \frac{K(0)}{\beta_1 t^{1/2}} = \frac{K_0}{t^{1/2}\sqrt{-2(K_0 - K_i)\Big/\int_{\theta_i}^{\theta_0} h d\theta}}$$

Neglecting the small value of K_i, the above equation becomes

$$q_0 = \frac{\sqrt{-2K_0\int_{\theta_i}^{\theta_0} h d\theta}}{2t^{1/2}}, \quad [13]$$

The cumulative infiltration $i(t)$ is the integral of Eq. [4] between the boundaries q_i and q_0.

$$i(t) = \int_{\theta_i}^{\theta_0} x d\theta = \beta_1 t^{1/2}\int_{\theta_i}^{\theta_0} h d\theta \quad [14]$$

And taking the derivative of the above equation also defines the infiltration rate at the soil surface $q_0(t)$

$$q_0(t) = \frac{\beta_1\int_{\theta_i}^{\theta_0} h d\theta}{2t^{1/2}}$$

Substituting b_1 into the above equation, we have

$$q_0(t) = \frac{\sqrt{-2(K_0 - K_i)\int_{\theta_i}^{\theta_0} h d\theta}}{2t^{1/2}}$$

which is identical to Eq. [13] when the small value of K_i is again neglected.

Graphs illustrating Eqs. [9 through 13] are presented next for water infiltrating into the marine sand according to the similarity assumption that satisfies Eq. [1] with N = 1. Soil water content distributions within the profile at infiltration times of 15, 60 and 300 min obtained from Eq. [9] and the soil water retention function $q(h)$ are presented in Figure 2. The graphs terminate at values of the leading edge of the wetting front x_i, the smallest distance at which q is slightly greater than q_i.

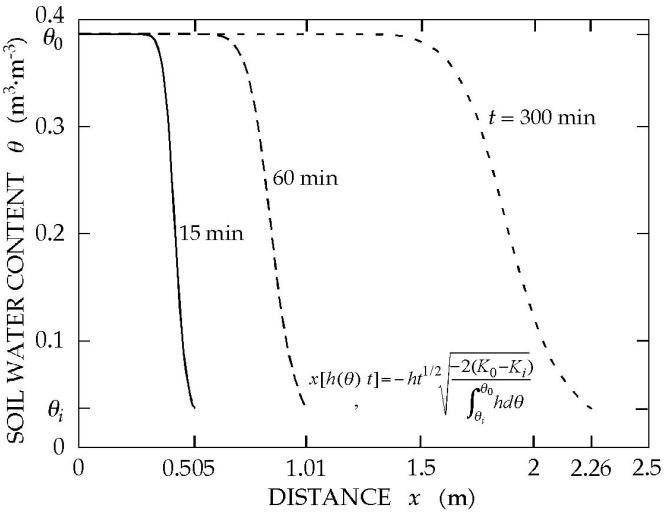

Figure 2. Soil water content distributions within the marine sand from the similarity solution satisfying the classical Boltzmann transform having exponent $N = 1$.

In Figure 3, graphs of matric potential head h and hydraulic gradient $\partial h/\partial x$ within the marine sand are plotted from Eqs. [10] and [11], respectively. For each infiltration time, the matric potential head illustrated in Figure 3A is linearly related to soil distance having a constant value indicated by the hydraulic gradient illustrated in Figure 3B.

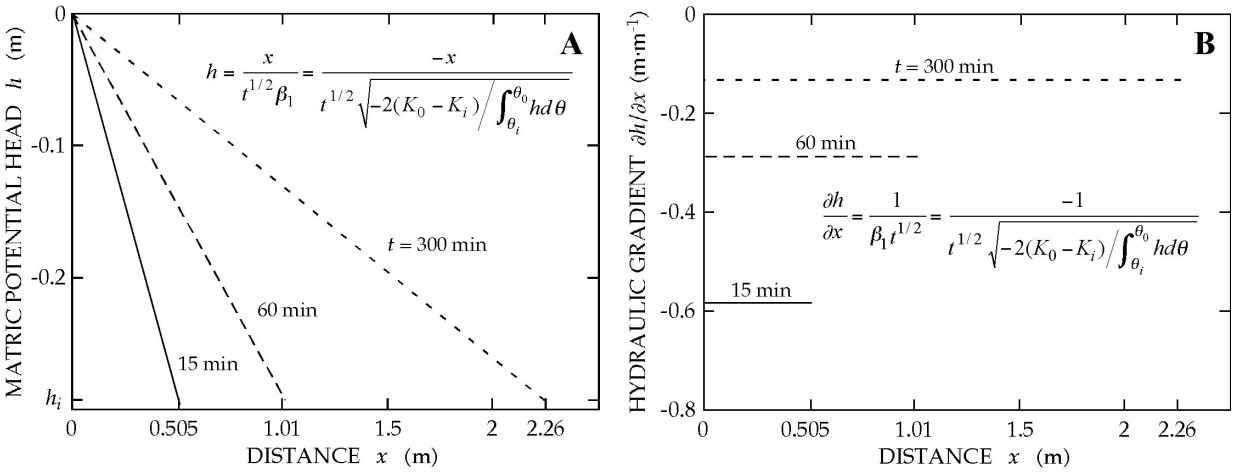

Figure 3. Matric potential head and hydraulic gradient within the marine sand from the similarity solution satisfying the classical Boltzmann transform having exponent $N = 1$.

In Figure 4, the soil water flux density q is plotted within the soil profile as well as the infiltration rate into the soil surface is plotted versus infiltration time from Eqs. [12] and [13],

respectively. Note, as expected, the water flux density diminishes to zero at the leading edge of the wetting front x_i,

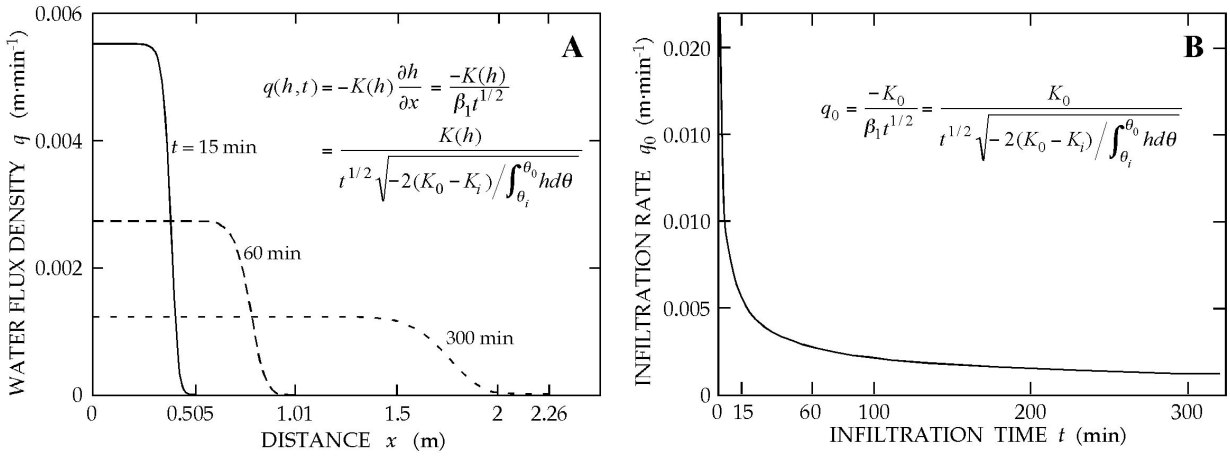

Figure 4. Water flux density within the marine sand and infiltration rate at its surface as a function of time from the similarity solution satisfying the classical Boltzmann transform having exponent $N = 1$.

For any constant value $h_j = h(q_j)$ Eq. [9] becomes

$$x(h_j,t) = \sqrt{-2h^2(\theta_j)\cdot(K_0 - K_i)\Big/\int_{\theta_i}^{\theta_0} h\,d\theta}\cdot t^{1/2} \qquad [15]$$

from which we illustrate in Figure 5 that the value of x increases linearly with the square root of time having a slope equal to

$$\sqrt{-2h^2(\theta_j)\cdot(K_0 - K_i)\Big/\int_{\theta_i}^{\theta_0} h\,d\theta}.$$

For $h_j = h_0 = 0$ the slope is zero with $x(0, t)$ remaining zero for all times. When $h_j = h_i$, Eq. [15] becomes

$$x(h_i,t) = \sqrt{-2h_i^2(K_0 - K_i)\Big/\int_{\theta_i}^{\theta_0} h\,d\theta}\cdot t^{1/2}$$

Hence, the distance x at which h_i exists during infiltration is a finite value and never becomes infinity until $t \rightarrow \infty$.

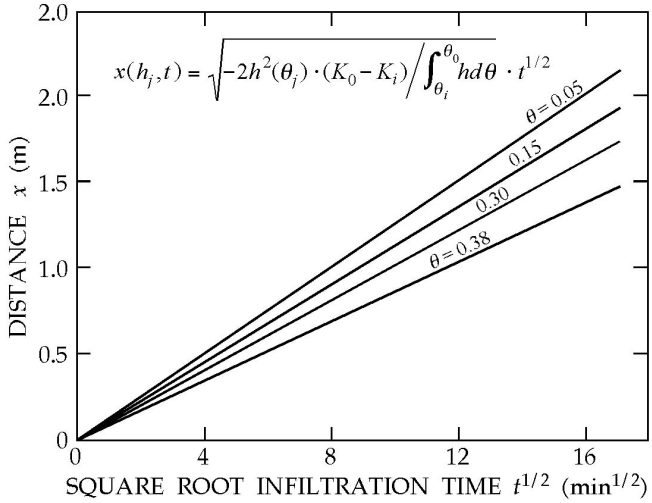

Figure 5. Distance from the surface of the marine sand that a given matric potential head proceeds within the sand profile as a function of the square root of infiltration time based on the similarity solution satisfying the Boltzmann transform having exponent $N = 1$.

Integrating integrals with definite limits

To ensure that the presentation above is without mathematical errors, we integrate Eq. [2] using definite limits for the boundary conditions of q_0 and q_i.

$$\int_{\lambda(h_i)}^{\lambda(h)} \frac{d\lambda}{\lambda} = \int_{h_i}^{h} \frac{dh}{h} \qquad [16]$$

We obtain

$$\ln\lambda(h) - \ln\lambda(h_i) = \ln h - \ln h_i$$

which becomes

$$\frac{\lambda(h)}{\lambda(h_i)} = \frac{h}{h_i} \quad \text{or} \quad \frac{h}{\lambda(h)} = \frac{h_i}{\lambda(h_i)} \qquad [17]$$

and reduces to

$$\lambda(h) = \frac{\lambda(h_i)}{h_i} h \qquad [18]$$

Recognizing that $\lambda(h) = xt^{-1/2}$, the above equation becomes

$$x(h,t) = \frac{\lambda(h_i)}{h_i} h t^{1/2} \qquad [20]$$

Holding x constant with respect to t, we take the partial derivative of Eq. [20] with respect to t

$$\frac{\partial h}{\partial t} = -\frac{h}{2t} \qquad [21]$$

Holding t constant with respect to x, we take the partial derivative of Eq. [20] with respect to x

$$\frac{\partial h}{\partial x} = \frac{h_i}{\lambda(h_i)t^{1/2}} \qquad [22]$$

Holding t constant with respect to x, we take the partial derivative of Eq. [22] to obtain

$$\frac{\partial^2 h}{\partial x^2} = 0 \qquad [23]$$

Substituting Eqs. [21, 22 and 23] into Eq. [3], we obtain

$$-\frac{\lambda^2(h_i)h}{2h_i^2}\frac{d\theta}{dh} = \frac{dK(h)}{dh}$$

Multiplying by Dh and integrating using definite limits for the boundary conditions of q_0 and q_i, we have

$$-\frac{\lambda^2(h_i)}{2h_i^2}\int_{\theta_i}^{\theta_0} h d\theta = \int_{K_i}^{K_0} dK$$

which simplifies to

$$\lambda(h_i) = -\sqrt{-2(K_0 - K_i)\Big/\int_{\theta_i}^{\theta_0} h d\theta}\cdot h_i$$

Substituting the above equation into Eq.[18], we obtain

$$x(h,t) = -ht^{1/2}\sqrt{-2(K_0 - K_i)\Big/\int_{\theta_i}^{\theta_0} h d\theta} \qquad [24]$$

which is identical to Eq. [9].

From the above, we are assured that the similarity solution satisfying the classical Boltzmann transform having exponent N = 1 has been uniquely developed. Although the solution provides estimates that are not exact physical realities, it can be used directly without any arbitrary curve fitting or estimations of any kind of a mean value within the wetting profile of the marine sand as was done by Prevedello et al. (2008 and 2009).

Annotation of Similarity Solution Using Extended Boltzmann Transform l^2

Integrating integrals with indefinite limits

In the same manner as Prevedello et al. (2008), we begin by selecting an exponent of $N = 2$ for l in Eq. [1] to annotate their similarity solution. Eq. [1] mathematically equivalent to

$$\frac{d\lambda^2}{\lambda^2} = \frac{dh}{h} \qquad [25]$$

is integrated with indefinite integrals

$$\int \frac{d\lambda^2}{\lambda^2} = \int \frac{dh}{h} + \ln \beta_2$$

to yield

$$\lambda^2 = \beta_2 h \qquad [26]$$

where β_2 is a constant of integration having a value dependent upon the boundary conditions of both *l* and *h*. Recognizing that $\lambda[\theta(h)] = xt^{-1/2}$, Eq. [26] becomes

$$x = \sqrt{\beta_2 ht} \qquad [27]$$

The partial derivative of Eq. [27] with respect to *t* holding *x* constant is

$$\frac{\partial h}{\partial t} = -\frac{h}{t} \qquad [28]$$

The partial derivative of Eq. [27] with respect to *x* holding *t* constant is

$$\frac{\partial h}{\partial x} = \frac{2x}{\beta_2 t} \qquad [29]$$

The partial derivative of Eq. [29] with respect to *x* holding *t* constant is

$$\frac{\partial^2 h}{\partial x^2} = \frac{2}{\beta_2 t} \qquad [30]$$

To ascertain the value of b_2, when the partial derivatives in Eqs. [28, 29 and 30] are substituted into Eq. [3], we obtain

$$-\frac{h}{t}\frac{d\theta}{dh} = \frac{2}{\beta_2 t} K(h) + \left(\frac{2x}{\beta_2 t}\right)\left(\frac{2x}{\beta_2 t}\right)\frac{dK(h)}{dh}$$

which simplifies to

$$\beta_2 h \frac{d\theta}{dh} = -2K(h) - 4h\frac{dK(h)}{dh} \qquad [31]$$

The above equation multiplied by *Dh* to prepare for its integration between boundary conditions q_i and q_0 becomes

$$\beta_2 h \frac{d\theta}{dh}\Delta h = -2K(h)\Delta h - 4h\frac{dK(h)}{dh}\Delta h$$

Integrating, we have

$$\beta_2 \int_{\theta(h_i)}^{\theta(h_0)} h d\theta = -2 \int_{h_i}^{h_0} K(h) dh - 4 \int_{K(h_i)}^{K(h_0)} h dK$$

which reduces to

$$\beta_2 \int_{\theta(h_i)}^{\theta(h_0)} h d\theta = 2 \int_{h_i}^{h_0} K dh$$

Hence,

$$\beta_2 = 2 \int_{h_i}^{h_0} K dh \Big/ \int_{\theta(h_i)}^{\theta(h_0)} h d\theta \qquad [32]$$

Substituting b_2 into Eq. [27], we obtain

$$x(h,t) = \sqrt{2h \int_{h_i}^{h_0} K dh \Big/ \int_{\theta(h_i)}^{\theta(h_0)} h d\theta} \cdot t^{1/2} \qquad [33]$$

from which we ascertain $h(x,t)$

$$h = \frac{x^2}{t\beta_2} = \frac{x^2}{2t \int_{h_i}^{h_0} K dh \Big/ \int_{\theta(h_i)}^{\theta(h_0)} h d\theta} \qquad [34]$$

to quantify the mean of $h(x,t)$ from the soil surface to any distance x within the wetting soil profile

$$\bar{h}_x = \int_0^x h dx \Big/ \int_0^x dx = \frac{1}{x} \int_0^x \frac{x^2}{\beta_2 t} dx = \frac{x^2}{3\beta_2 t} \qquad [35]$$

Holding t constant in Eq. [34], the partial derivative of h with respect to x is

$$\frac{\partial h}{\partial x} = \frac{2x}{t\beta_2} = \frac{x}{t \int_{h_i}^{h_0} K dh \Big/ \int_{\theta(h_i)}^{\theta(h_0)} h d\theta} \qquad [36]$$

The mean water flux density within the soil profile at any time as well the infiltration rate at the soil surface as a function of time can be readily ascertained from the mean of $\partial h / \partial x$ from the soil surface to a distance x within the wetting soil profile is

$$\overline{\frac{\partial h}{\partial x}} = \int_0^x \frac{\partial h}{\partial x} dx \Big/ \int_0^x dx = \frac{1}{x} \int_0^x \frac{2x}{t\beta_2} dx = \frac{x}{t\beta_2} \qquad [37]$$

The mean water flux density $\bar{q}(x,t)$ within the wetting soil profile to a distance x is

$$\bar{q}(x,t) = -\bar{K}_x \overline{\frac{\partial h}{\partial x}} = -\bar{K}_x \frac{x}{t\beta_2} \qquad [38]$$

where

$$\bar{K}_x = \frac{1}{x} \int_0^x K dx.$$

The cumulative infiltration $i(t)$ at the soil surface is the integral of Eq. [33] between the boundary conditions q_i and q_0

$$i(t) = \int_{\theta_i}^{\theta_0} x d\theta = t^{1/2} \sqrt{-2\int_{h_i}^{h_0} K dh \Big/ \int_{\theta(h_i)}^{\theta(h_0)} h d\theta} \cdot \int_{\theta_i}^{\theta_0} |h|^{1/2} d\theta$$

Hence,

$$i(t) = t^{1/2} \sqrt{-2\int_{h_i}^{h_0} K dh \Big/ \int_{\theta(h_i)}^{\theta(h_0)} h d\theta} \cdot \int_{\theta_i}^{\theta_0} |h|^{1/2} d\theta \qquad [39]$$

Taking the derivative of the above equation defines the infiltration rate at the soil surface $q_0(t)$

$$q_0(t) = \frac{\int_{\theta_i}^{\theta_0} |h|^{1/2} d\theta \sqrt{-2\int_{h_i}^{h_0} K dh \Big/ \int_{\theta(h_i)}^{\theta(h_0)} h d\theta}}{2t^{1/2}} \qquad [40]$$

Using the hydraulic parameters of the marine sand published by Prevedello et al. (2008, 2009) with q_i and q_0 being 0.037 and 0.387, respectively, we next present graphs illustrating Eqs. [33, 35, 37, 38 and 40]. Soil water content distributions within the profile at infiltration times of 15, 60 and 300 min obtained from Eq. [33] and the soil water retention function $q(h)$ are presented in Figure 6. Again, the graphs terminate at values of the leading edge of the wetting front x_i, the smallest distance at which q is greater than q_i.

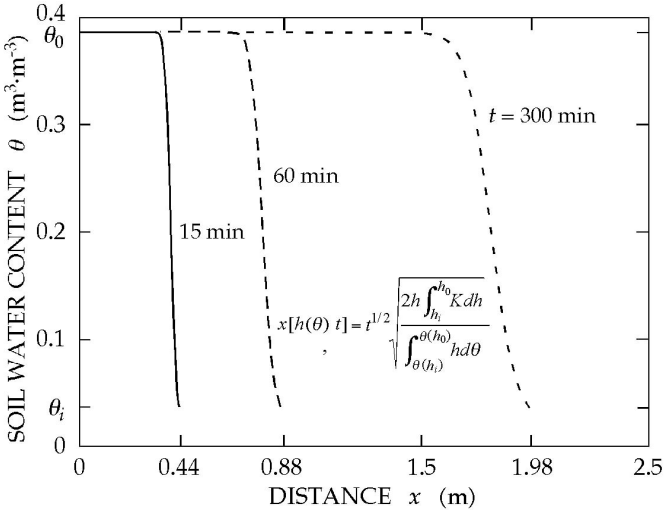

Figure 6. Soil water content distributions within the marine sand from the similarity solution satisfying the extended Boltzmann transform having exponent $N = 2$.

In Figure 7, graphs of mean matric potential head $\bar{h}$ and mean hydraulic gradient $\overline{\partial h / \partial x}$ within the soil profile are plotted from Eqs. [35] and [37], respectively. For each infiltration time, the mean

matric potential head illustrated in the left-hand graph is parabolically related to soil distance yields a constant mean value of the hydraulic gradient illustrated in the right-hand graph.

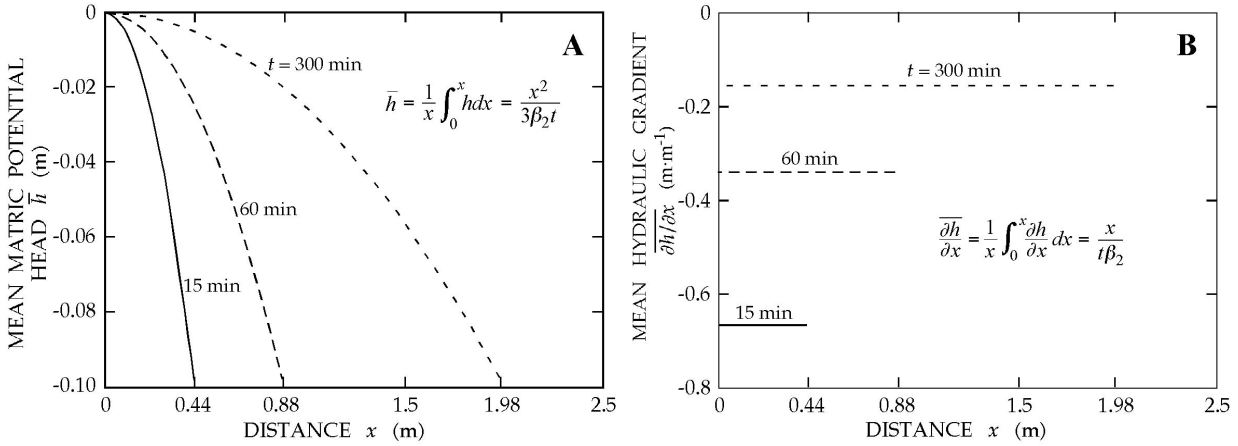

Figure 7. Mean matric potential head and mean hydraulic gradient within the marine sand from the similarity solution satisfying the extended Boltzmann transform having exponent $N = 2$.

In Figure 8, the mean water flux density $\bar{q}$ is plotted within the soil profile as well as the infiltration rate into the soil surface is plotted versus infiltration time from Eqs. [38] and [40], respectively.

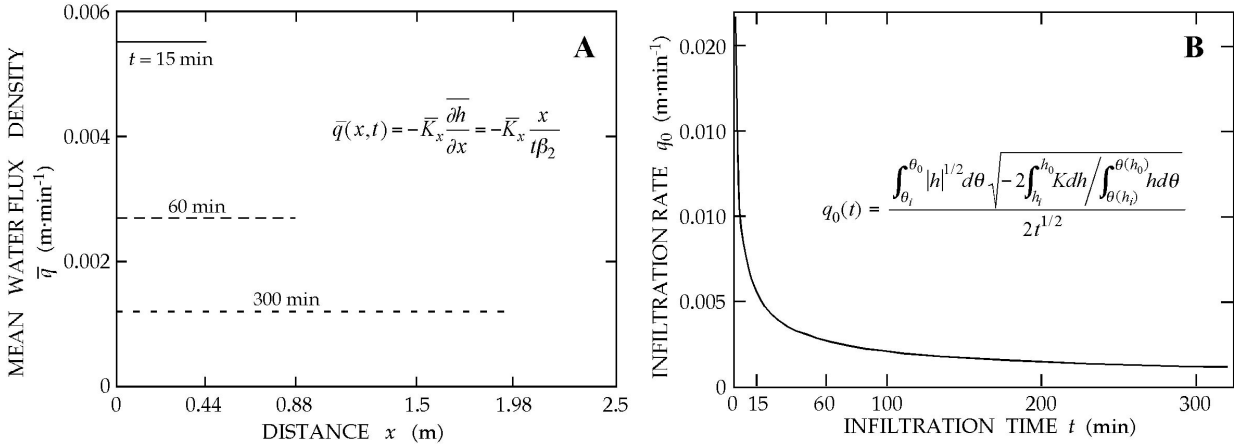

Figure 8. Mean water flux density within the marine sand and infiltration rate at its surface as a function of time from the similarity solution satisfying the extended Boltzmann transform having exponent $N = 2$.

The similarity solution based on the extended Boltzmann transform (N = 2) allows the estimation of the mean matric potential head, the mean hydraulic gradient and the mean water flux density across the wetting soil profile to any distance as well as the infiltration rate at the soil surface as a function of time. Calculating these mean values is easily achieved with a reliably computed value of b_2. We emphasize here that the value of b_2 from Eq. [32] differs substantially from that calculated from the equation

$$\beta_2 = -\frac{2K_0}{\theta_0 - \theta_i}$$

published as Eq. [20] in Prevedello et al. (2008). We note that all of the mathematical and physically related development presented above in this document and that in Prevedello et al. (2008) yielded identically the same differential equation to be integrated to obtain the value of b_2. That is, Eq. [31] above and Eq. [17] in Prevedello et al. (2008) are identical before they were integrated between the boundary limits of $q(h_i)$ and $q(h_0)$. During the integration of the last term of Eq. [17] in Prevedello et al. (2008), both its integrand and limits of integration were modified and are different from those integrated in Eq. [8] above. Hence, which equation – Eq. [32] above or Eq. [20] in Prevedello et al. (2008). – is the more analytically reliable to quantify and test the results of the similarity hypothesis based on the extended Boltzmann transform with an exponent of 2? To answer this question, we return to Eq. [2] and integrate it with definite limits avoiding the necessity of explicitly ascertaining the value of b_2 in Eq. [3] that is a constant having a value dependent upon the boundary conditions of both l and $q(h)$.

Integrating integrals with definite limits for N = 2

Integrating Eq. [25] with definite limits,

$$\int_{\lambda(h_i)}^{\lambda(h)} \frac{d\lambda^2}{\lambda^2} = \int_{h_i}^{h} \frac{dh}{h} \qquad [41]$$

we obtain

$$\ln \lambda^2(h) - \ln \lambda^2(h_i) = \ln h - \ln h_i$$

which becomes

$$\frac{\lambda^2(h)}{\lambda^2(h_i)} = \frac{h}{h_i} \quad \text{or} \quad \frac{h}{\lambda^2(h)} = \frac{h_i}{\lambda^2(h_i)} \qquad [42]$$

and reduces to

$$\lambda^2(h) = \frac{\lambda^2(h_i)}{h_i} h \qquad [43]$$

Recognizing that $\lambda(h) = xt^{-1/2}$, the above equation becomes

$$x(h,t) = \frac{\lambda(h_i)}{h_i^{1/2}} \cdot h^{1/2} \cdot t^{1/2} \quad \text{or} \quad x(h,t) = \lambda(h_i) \frac{(-h)^{1/2}}{(-h_i)^{1/2}} t^{1/2} \qquad [44]$$

The partial derivative of Eq. [44] with respect to *t* holding *x* constant is

$$\frac{\partial h}{\partial t} = -\frac{h}{t} \qquad [45]$$

The partial derivative of Eq. [44] with respect to *x* holding *t* constant is

$$\frac{\partial h}{\partial x} = \frac{2h^{1/2} h_i^{1/2}}{\lambda(h_i) t^{1/2}} \qquad [46]$$

The partial derivative of Eq. [46] with respect to *x* holding *t* constant is

$$\frac{\partial^2 h}{\partial x^2} = \frac{2h_i^{1/2}}{\lambda(h_i) t^{1/2}} \cdot \frac{1}{2h^{1/2}} \frac{\partial h}{\partial x} = \frac{2h_i^{1/2}}{\lambda(h_i) t^{1/2}} \cdot \frac{1}{2h^{1/2}} \frac{2h^{1/2} h_i^{1/2}}{\lambda(h_i) t^{1/2}}$$

which reduces to

$$\frac{\partial^2 h}{\partial x^2} = \frac{2h_i}{\lambda^2(h_i) t} \qquad [47]$$

Substituting Eqs.[45, 46 and 47] into Eq. [3], we obtain the step-wise sequence of equations

$$-\frac{h}{t}\frac{d\theta}{dh} = \frac{2h_i}{\lambda^2(h_i)t} K(h) + \frac{4hh_i}{\lambda^2(h_i)t} \frac{dK(h)}{dh}$$

$$-h\lambda^2(h_i)\frac{d\theta}{dh} = 2h_i K(h) + 4hh_i \frac{dK(h)}{dh}$$

$$-\frac{h\lambda^2(h_i)}{h_i}\frac{d\theta}{dh} = 2K(h) + 4h\frac{dK(h)}{dh}$$

$$-\frac{\lambda^2(h_i)}{h_i} h \frac{d\theta}{dh} \Delta h = 2K(h)\Delta h + 4h\frac{dK(h)}{dh}\Delta h$$

$$-\frac{\lambda^2(h_i)}{h_i}\int_{\theta_i}^{\theta_0} h\,d\theta = 2\int_{h_i}^{h_0} K dh + 4\int_{K_i}^{K_0} h dK$$

$$-\frac{\lambda^2(h_i)}{h_i}\int_{\theta_i}^{\theta_0} h\,d\theta = 2\int_{h_i}^{h_0} K dh - 4\int_{h_i}^{h_0} K dh$$

$$-\frac{\lambda^2(h_i)}{h_i}\int_{\theta_i}^{\theta_0} h\,d\theta = -2\int_{h_i}^{h_0} K dh$$

$$\lambda^2(h_i) = -h_i\left(-2\int_{h_i}^{h_0} Kdh \Big/ \int_{\theta_i}^{\theta_0} hd\theta\right)$$

$$\lambda(h_i) = (-h_i)^{1/2}\sqrt{-2\int_{h_i}^{h_0} Kdh \Big/ \int_{\theta_i}^{\theta_0} hd\theta}$$

Substituting the above equation into Eq. [44], we obtain

$$x(h,t) = \sqrt{2h\int_{h_i}^{h_0} Kdh \Big/ \int_{\theta_i}^{\theta_0} hd\theta}\cdot t^{1/2} \qquad [48]$$

that is identical to Eq. [33] derived by integrating Eq. [25] using indefinite integrals. Obtaining this identity, we conclude that the value of b_2 from Eq. [32] is more reliable than that published in Prevedello et al. (2008).

A Brief Addendum to the Publication of Prevedello et al. (2009)

In the publication of Prevedello et al. (2009), they stated that their similarity hypothesis was similar but not the same as that of Prevedello et al. (2008). Later, Prevedello and Loyola (2010) stated that the similarity solution of Prevedello et al. (2009) presumes a Boltzmann relation of l equal to $C_1 h$. These two statements establish an ambiguity that we now clarify. Except for a few typographical errors, the equations in the 2009 publication are mathematically correct and yield the similarity solution

$$x(h,t) = \sqrt{\frac{-2(K_0 - K_i)ht}{(\theta_0 - \theta_i)}} \qquad [49]$$

that satisfies the assumption that

$$x\frac{\partial\theta}{\partial x} = h\frac{d\theta}{dh}. \qquad [50]$$

without invoking a Boltzmann transform. ANA ARRUMAR

The cumulative infiltration I is easily determined by integrating Eq. [49] between the limits of Θ_i and Θ_0

$$I(t) = \sqrt{\frac{2(K_0 - K_i)}{(\theta_0 - \theta_i)}}\int_{\theta_i}^{\theta_0} |h|^{1/2} d\theta\cdot t^{1/2} \qquad [51]$$

Taking the derivative of the above equation also defines the infiltration rate at the soil surface $q_0(t)$

$$q_0(t) = \sqrt{\frac{(K_0 - K_i)}{2(\theta_0 - \theta_i)}}\int_{\theta_i}^{\theta_0} |h|^{1/2} d\theta\cdot\frac{1}{t^{1/2}} \qquad [52]$$

It is apparent that Eq. [49] is not identical to Eq. [9] (or Eq. [24]) because the latter was derived with the classical Boltzmann transform

$$\lambda \frac{d\theta}{d\lambda} = h \frac{d\theta}{dh} \qquad [53]$$

Similarities imposed by Eqs. [50] and [53] on the solution of Richards' equation are not equivalent.

Classical Solution of Richards' Equation – A Reminder of Reality

With the above three similarity solutions each being based on different assumptions, each of them offers a different approximation to physical reality. Seeking criteria to optimize their potential acceptability for not only the marine sand but also for other soils, we now compare each of their solutions with that of a classic solution of Richards' equation provided by Philip (1955). Soil water content distributions within the profile at infiltration times of 15, 60 and 300 min presented in Figure 9 theoretically embrace a value of q_i only at a distance x as it approaches infinity and are less sigmoid shaped than the three similarity solutions. In Figure 10A we observe that the classically obtained matric potential head is not entirely linear with distance as it is in Figure 3A calculated for a similarity hypothesis assuming an exponent $N = 1$. And we also observe in Figure 10B that the hydraulic gradient is not constant with distance as it is in Figure 3B. Near the wetting front the classical water flux density shown in Figure 11A decreases more abruptly than that illustrated in Figure 4A.

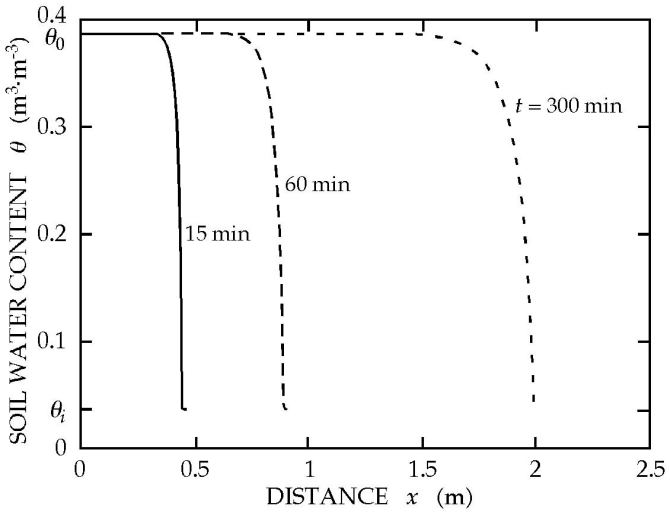

Figure 9. Physically realistic soil water content distributions within marine sand obtained from a classical solution of Richards' equation.

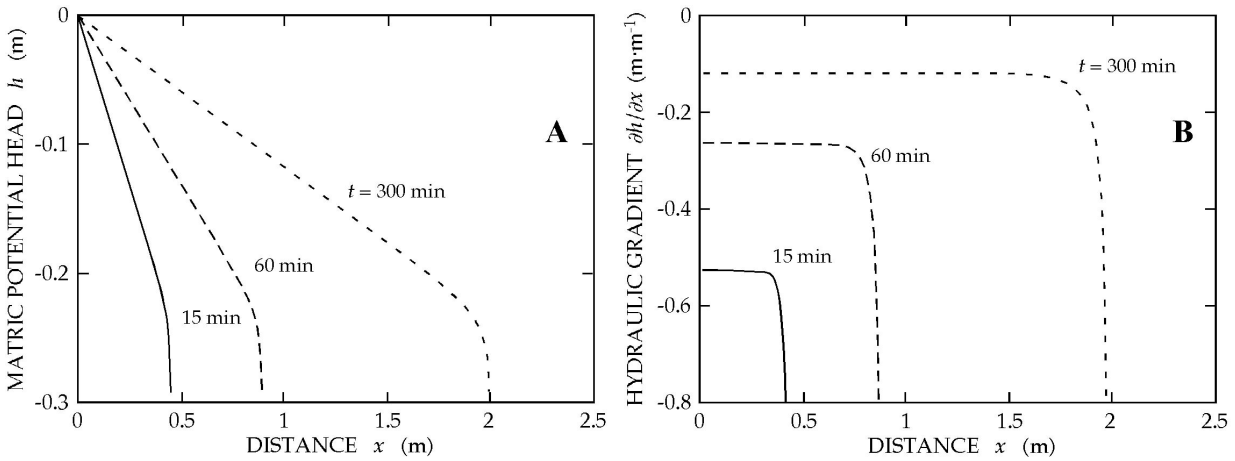

Figure 10. Matric potential head and hydraulic gradient within marine sand obtained from a classical solution of Richards' equation.

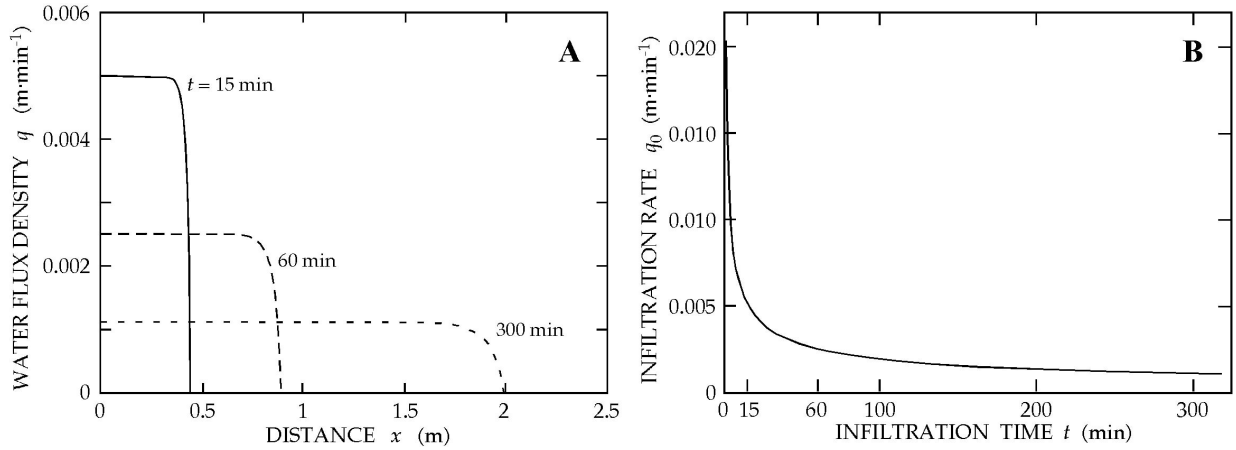

Figure 11. Water flux density within soil profile and infiltration rate at the soil surface as a function of time for marine sand obtained from a classical solution of Richards' equation.

Although the infiltration rate versus time graphs presented in Figures 4B, 8B and 11B appear identical, they are each different as can be observed in Figure 12 where the cumulative infiltration for the three similar hypotheses and that for the classical solution of Richards' equation are each plotted as a function of square root of time. Although all three cumulative infiltration calculations stemming from similarity hypotheses over-estimate reality, they are in virtual agreement for any typical rainfall or irrigation event that provides up to about 20 cm of water entering the soil surface.

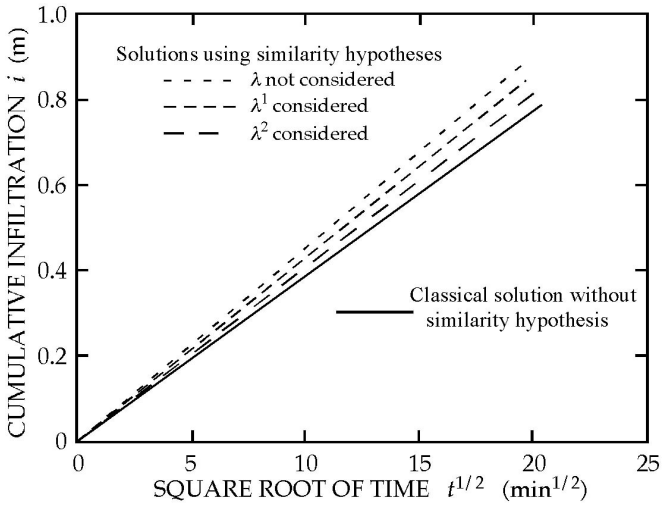

Figure 12. Graphs of cumulative infiltration versus square root of time from Eqs. [14, 39 and 51] and that from the classical solution of Richards' equation.

After presenting the above similarity solutions of infiltration derived from Richards' equation for the marine sand, we make the following assertions:

1. None of the three similarity solutions are identical to each other Although that satisfying the extended Boltzmann transform with exponent N = 2 is closest to reality, none of them match the traditional solution of Richards' equation.
2. After infiltration begins at $t > 0$, classical solutions predict that the initial soil water content q_i exists only at a distance x equal to infinity. In contrast, the three similarity solutions reveal that q_i exists at finite distances that increase with time. To date, typical experiments commonly reveal that values of q not measureably greater q_i exist at relatively short distances ahead of the measured wetting front and are not uniquely restricted to the immeasurable theoretical distance of infinity.
3. Without the necessity of calculating mean values of any term (q, h, $\partial h/\partial x$, K or x), the similarity solution based on the classical Boltzmann transform ($N = 1$) can be used directly to approximate the hydraulic gradient and the water flux density within the soil profile as well as the infiltration rate at the soil surface as a function of time. In this case, the similarity hypothesis with N=1 is close to reality because of the astonishingly abrupt, step-function shape of $q(h)$ – with an increase of less than 10 cm in the matric potential head h, the soil water content increases from virtually air-dryness to nearly water saturation (e.g., from 0.037 to 0.377 cm^3/cm^3).

4. The mean hydraulic gradient calculated from the similarity solutions based on the extended Boltzmann transform (N=2) and that of Prevedello (2009) can be used to estimate the mean water flux density within the soil profile as well the infiltration rate at the soil surface as a function of time.

Exploring the Utility of Similarity Solutions to Estimate Horizontal Infiltration into Soils of Different Textures and Amounts of Aggregated Particles

The Green and Ampt equation, initially published in 1911 for its application to sandy soils, has now been successfully used for all kinds of soils. Inasmuch as Green and Ampt did not theoretically quantify their assumed "value of the matric potential head at the wetting front", they designated it as a parameter to be empirically evaluated from observations recorded during infiltration experiments. Hence, for a century without a better theoretical basis, such observations have linked the "piston flow" of water through the "water-saturated transmission zone" of soil profiles. We now explore how well the Prevedello similarity hypotheses predict infiltration into two finer-textured soils based on a prior knowledge of $K(q)$ and $q(h)$ without depending upon an empirically determined value of h at the "so-called" wetting front. The hydraulic properties of the two soils – Columbia silt loam and Hesperia sandy loam – are given in Table 1.

Table 1. Saturated hydraulic conductivity K_0, saturated volumetric water content q_0, residual volumetric water content q_r and van Genuchten (1980) wetting parameters a, l, m and n for Columbia silt loam and Hesperia sandy loam (Nielsen et al., 1962)

Soil	K_0	q_0	q_r	a	l	m	n
	cm/min	cm^3/cm^3	cm^3/cm^3	1/cm			
Columbia	0.0464	0.450	0.020	0.01185	0.50	0.5078	2.032
Hesperia	0.1140	0.385	0	0.03250	1.77	0.3506	1.540

The wetting parameters are those defined in the van Genuchten-Mualem model (van Genuchten, 1980) for the soil water retention function

$$S_e = \frac{\theta(h) - \theta_r}{\theta_0 - \theta_r} = \frac{1}{(1 + |\alpha h|^n)^m} \qquad [54]$$

and the hydraulic conductivity

$$K(\theta) = K_0 S_e^{l}[1-(1-S_e^{1/m})^m]^2 \qquad [55]$$

where S_e is the effective volumetric water saturation, l the pore connectivity, and a, m and n are shape parameters. The initial and boundary conditions listed above in the introductory paragraph were experimentally established for each soil. The initial soil water content of the Columbia soil was 0.031 $cm^3 \cdot cm^{-3}$ while that of the Hesperia soil was 0.026 $cm^3 \cdot cm^{-3}$. Soil water content was measured at 1-cm intervals for three different infiltration times – 88, 344 and 740 min for the Columbia soil, and 158, 620 and 1467 min for the Hesperia soil (Nielsen et al., 1962).

Columbia silt loam

Soil water content distributions within Columbia silt loam at infiltration times of 88, 344 and 740 min obtained from the similarity solution Eq. [33] and the soil water retention function $q(h)$ are presented in Figure 13A. With Figure 13B showing the measured data together with the classical solution of Richards' equation, it is immediately obvious that the similarity solution estimates very gradual rather than very abrupt wetting fronts compared with those that are measured or calculated from the classical solution of Richards' equation. Visible in Figure 13A for an infiltration time of 88 min, the leading edge q_i of the wetting front reaches a distance of 87 cm. Not shown in the figure are the corresponding distances of 172 and 252 cm reached at the respective infiltration times of 344 and 740 min.

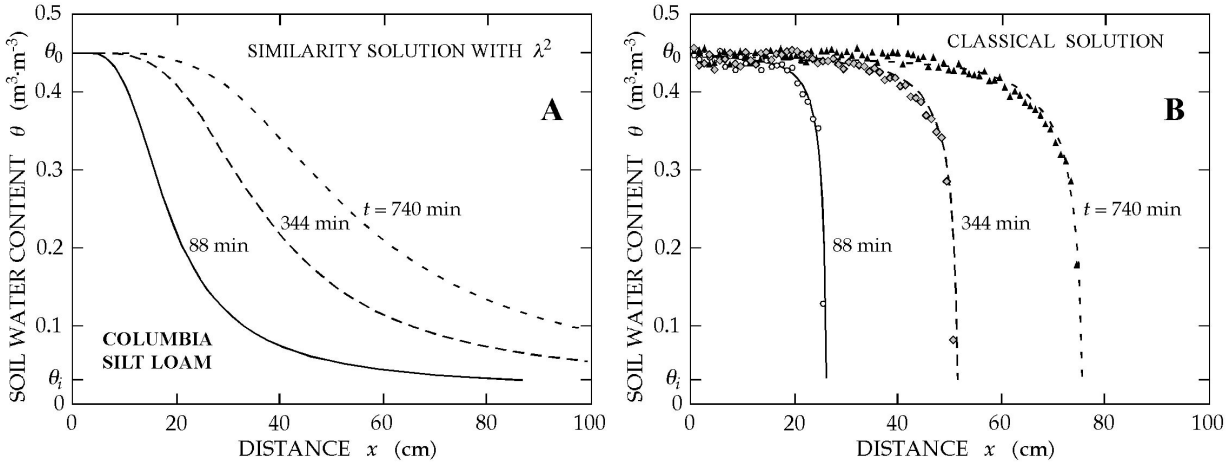

Figure 13. Soil water content distributions within Columbia silt loam from the similarity solution satisfying the extended Boltzmann transform having exponent N = 2, and those measured and calculated from classical solution of Richards' equation

Although the relative shapes of the soil water content distributions illustrated in Figures 13A and 13B for the same infiltration time are entirely different, the areas under each curve bounded by the lower limit of q_i are nearly identical. In other words, for a given time, the similarity solution (N = 2) and the classical solution each estimate nearly identical volumes of water entering into the soil surface. Hence, the cumulative infiltration estimated by both of these solutions are nearly identical as illustrated in Figure 14A. As expected and based on soil water content distributions within the soil profile not presented, the cumulative infiltration estimated from similarity solutions of Richards' equation using Eqs. [50] and [53] are entirely unrealistic. See Figure 14A. Illustrated in a different manner as graphs of infiltration rate versus infiltration time, the equivalent results are presented in Figure 14B.

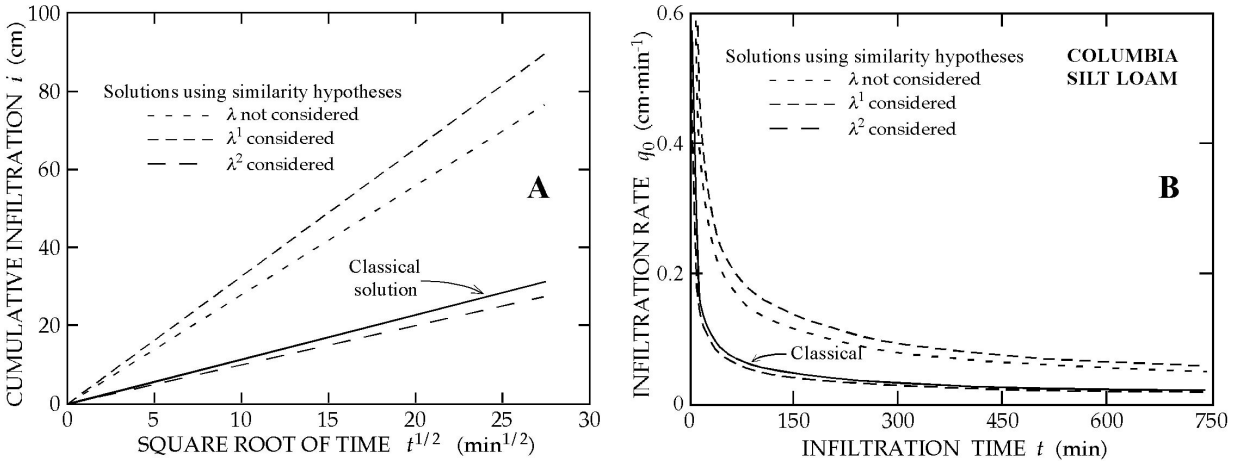

Figure 14. Infiltration rate into the surface of Columbia silt loam as a function of time from the similarity solution satisfying the extended Boltzmann transform having exponent N = 2, and that from the classical solution of Richards' equation.

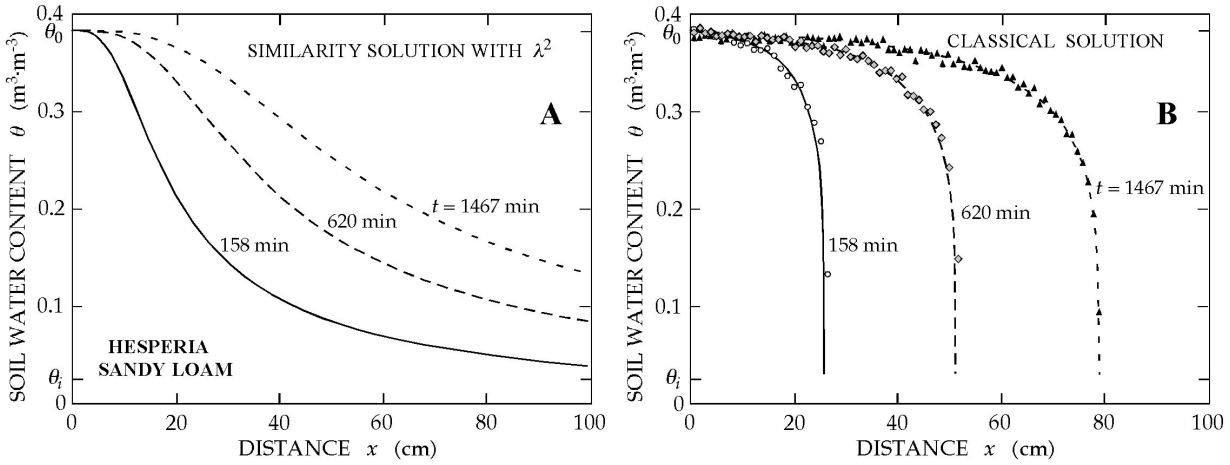

Figure 15. Soil water content distributions within Hesperia sandy loam from the similarity solution satisfying the extended transform having exponent N = 2, and those measured and calculated from classical solution of Richards' equation.

Hesperia sandy loam

Soil water content distributions within Hesperia sandy loam at infiltration times of 158, 620 and 1467 min obtained from the similarity solution Eq. [33] and the soil water retention function $q(h)$ are presented in Figure 15A. Comparable to the Columbia distributions (Figure 13A), the wetting fronts for Hesperia derived from the similarity solution are even more diffuse with their leading edge q_i reaching distances of 152, 301 and 464 cm that are not shown in the figure at corresponding infiltration times of 158, 620 and 1467 min. Figure 15B shows the measured data together with the classical solution. Also comparable to the Columbia results, the cumulative infiltration and infiltration rate functions in Figure 16 estimated from the similarity solution using the extended Boltzmann transform (N = 2) and the classical solution are virtually alike –the other two similarity solutions are not logical.

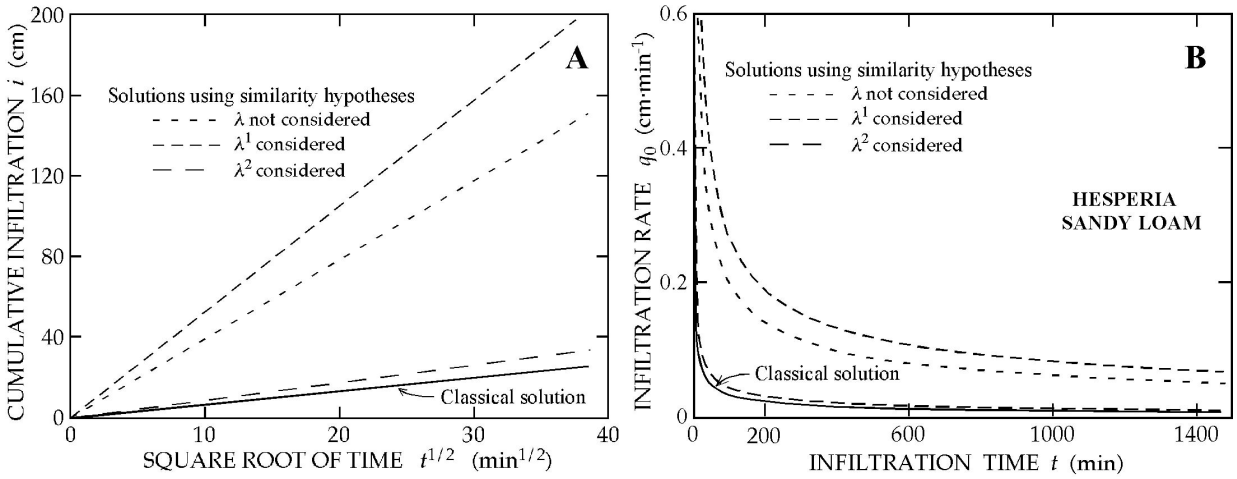

Figure 16. Infiltration rate into the surface of Hesperia sandy loam as a function of time from the similarity solution satisfying the extended Boltzmann transform having exponent $N = 2$, and that from the classical solution of Richards' equation.

PRESENT OUTLOOK

Without a comprehensive analysis of any additional infiltration experiments on a small or large number of natural-occurring soils each made with the aid of experimentally verified soil hydraulic properties, we tacitly predict that such research shall verify the beneficial utility of the innovative "Prevedello similarity solution" of Richards' equation. In other words, the empirical parameter identified as the matric potential head at the wetting front that is critical in the Green and Ampt analysis no longer needs to be ascertained or approximated. We anticipate that for any homogeneous soil, the horizontal infiltration process subject to the initial and boundary conditions of this presentation shall be adequately predicted by Eqs. [33]. [39] and [40].